Chapter 5

Operando Spectroscopic Analysis of CoP Films Electrocatalyzing the Hydrogen-Evolution Reaction

5.1 Introduction and Motivation

In the previous chapter, electrodeposited CoP films were demonstrated to effect the HER at a current density of -10 mA cm^{-2} with $-\eta < 100$ mV.[1] So far, however, characterization of this material, as well as related metal phosphides, has relied principally upon *ex-situ* techniques (analysis typically in vacuum or laboratory ambient). In this chapter, electrodeposited CoP films have been interrogated under *in-situ* and *operando* conditions using Raman spectroscopy and Co and P K-edge X-ray absorption spectroscopy (XAS).

5.2 Characterization of CoP films

5.2.1 Potentiostatic and ex-situ characterization of CoP films

CoP films were electrodeposited potentiostatically on planar Cu substrates, from an aqueous solution that contained $CoCl_2$ and $NaPO_2H_2$. Voltammetric, *in-situ,* and *operando* spectroscopic analyses were then performed in 0.500 M H_2SO_4(aq) (experimental methods are described in detail in Section 5.4). The steady-state voltammetric response indicated that production of cathodic current densities of 0.5 and

10 mA cm^{-2} required overpotentials of -34 and -92 mV (applied biases of -0.300 V and -0.358 V vs. a saturated calomel electrode [SCE]), respectively (Figure 5.1).

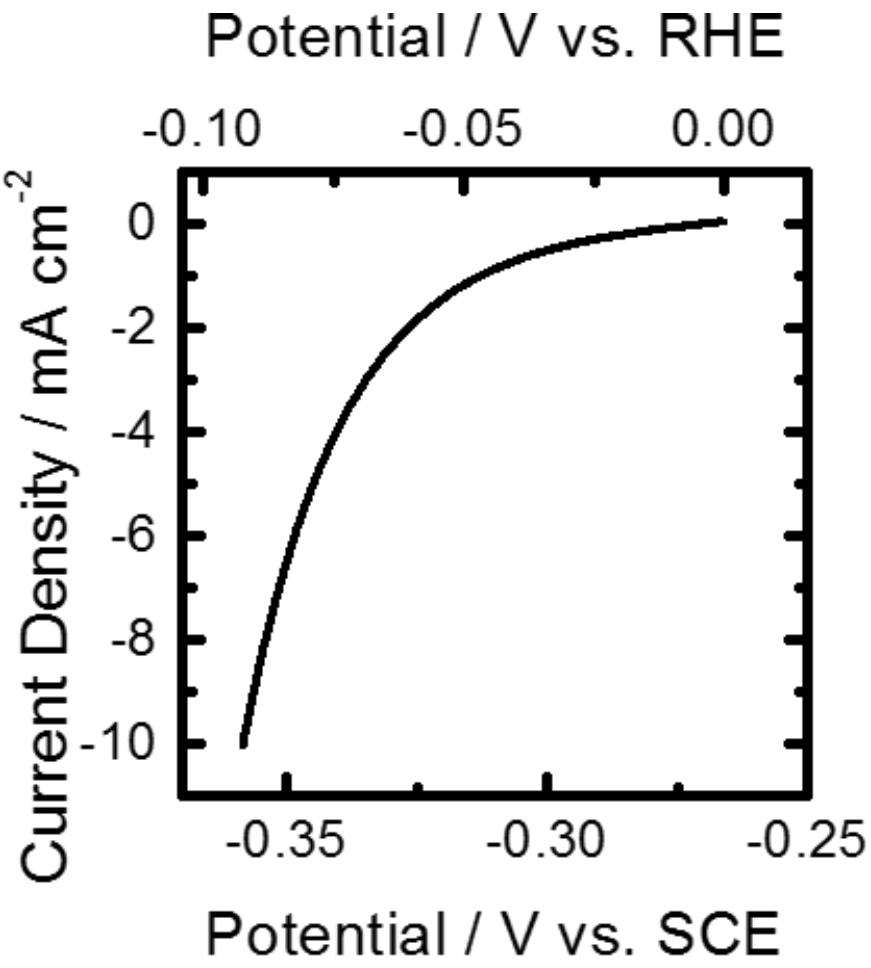

Figure 5.1: Cathodic polarization behavior of a CoP film in 0.500 M H_2SO_4(aq).

Figure 5.2a presents an *ex-situ* Raman spectrum collected from an as-deposited CoP film. A broad band centered at 595 cm^{-1} is indicative of amorphous cobalt oxide as it has been assigned in literature.[2] This band also exhibited shoulders at 477, 521, and 677 cm^{-1}, which correspond to Co_3O_4 phonon modes.[3] Several Raman modes were observed

in the 970-1200 cm^{-1} spectral region, and are consistent with P-O stretching vibrations in a disordered system.[4, 5] The presence of oxidized Co and P species in the as-prepared film is consistent with prior X-ray photoelectron spectroscopic (XPS) analysis performed in Chapter 4.

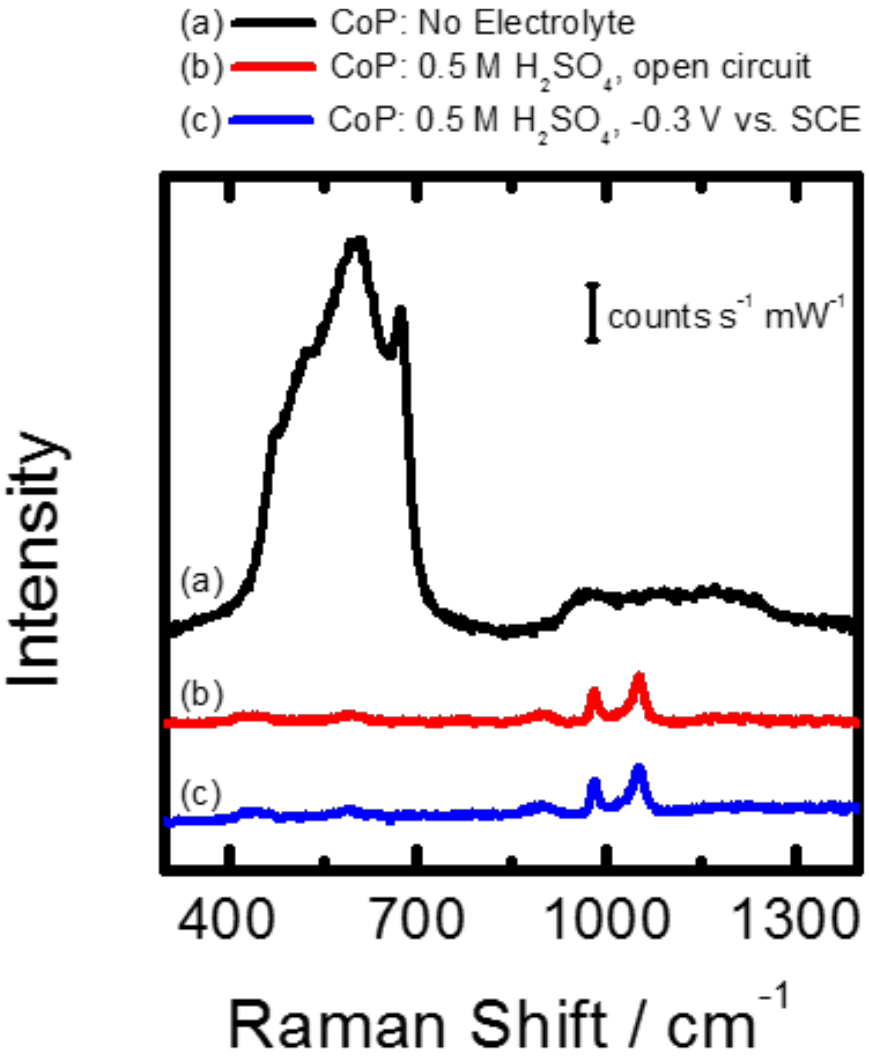

Figure 5.2: Raman spectra of CoP films acquired under the indicated conditions. (a) Ex-situ spectrum of a CoP film prior to contact with H_2SO_4(aq) (air ambient, ex-situ). (b) CoP film in 0.500 M H_2SO_4 (aq) at open circuit (in-situ). (c) Same as (b) but at an applied potential of -0.300 V vs. SCE (operando).

The same as-deposited CoP film was then immersed in 0.5 M H_2SO_4 (aq) and an *in-situ* Raman spectrum (open circuit condition) was collected while no externally applied bias was applied (Figure 5.2b). The observed Raman modes centered at 429, 587, 896, 980, 1054 cm^{-1} are consistent with scattering from the aqueous H_2SO_4 electrolyte.[6, 7] No other signals were observed, including those that correlate in the *ex-situ* Raman spectrum with oxidized Co and P species. After collection of the *in-situ* spectrum, a potential of -0.300 V vs. SCE was applied to the film such that the HER was being actively catalyzed and an *operando* Raman spectrum was acquired (Figure 5.2c). The *operando* spectrum was identical to the *in-situ* spectrum. Before and after collection of the both the *in-situ* and *operando* spectra, significant reflected excitation intensity was observed in a well-defined few-μm spot, consistent with the high numerical aperture of the objective in the Raman microprobe, indicating that the electrode interface was being interrogated during these analyses. The lack of observed phonon scattering in the *in-situ* and *operando* spectra is consistent with the amorphous nature of electrodeposited CoP materials and with the Pourbaix instability of oxidized cobalt species in strongly acidic media.[1, 8]

To more clearly identify the elemental oxidation states in the active electrocatalyst, Co K-edge and P K-edge XAS were performed in a manner analogous to the Raman investigation. Figure 5.3a-c presents representative *ex-situ*, *in-situ,* and *operando* Co K-edge XAS of electrodeposited CoP films collected in manner similar to the Raman spectra in Figure 5.2a-c. Figure 5.3d-e presents Co K-edge XAS of Co metal and CoO standard materials. The *ex-situ*, *in-situ,* and *operando* CoP spectra all share a

pre-edge feature near 7711 eV that is similar to, but less intense than, that in the Co metal standard. This feature is attributed to metal-to-ligand charge transfer, and resembles the pre-edge feature observed for Ni K-edge XAS of Ni_2P.[9, 10]

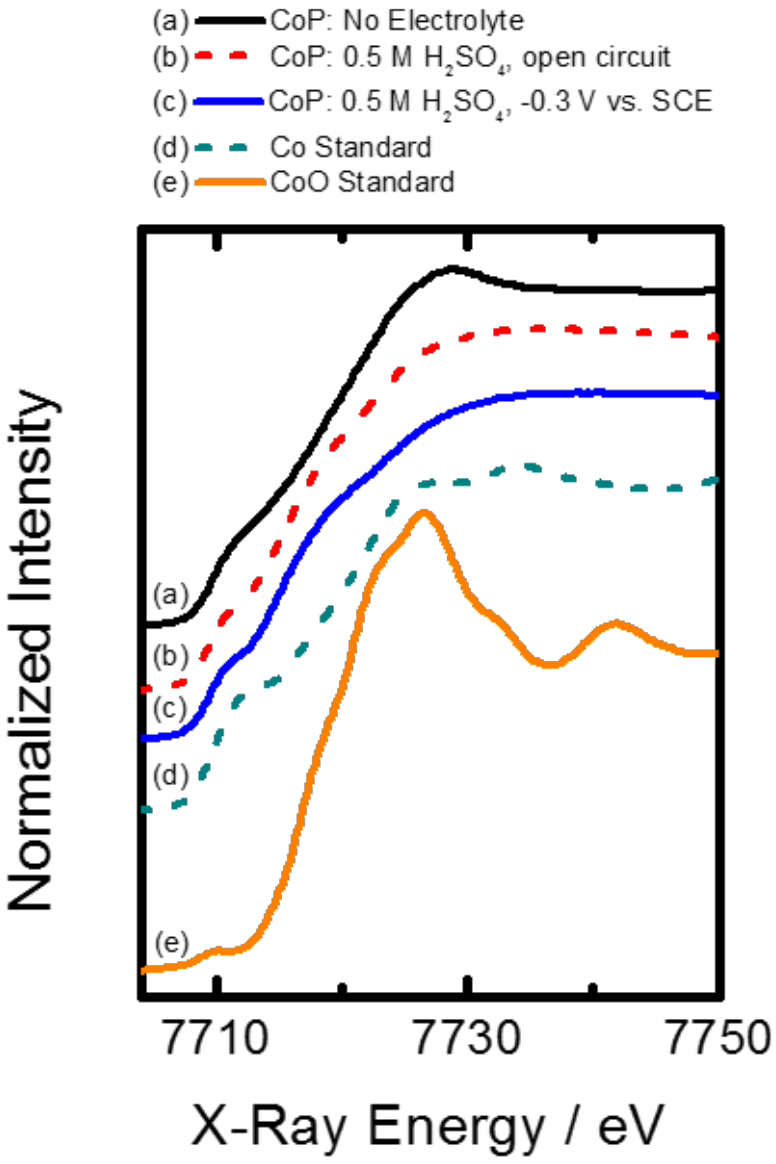

Figure 5.3: Co K-edge X-ray absorbance spectra of both CoP films under the indicated conditions and related spectral standards. (a) Ex-situ spectrum of a CoP film prior to contact with H_2SO_4(aq) (air ambient, ex-situ). (b) CoP film in 0.500 M H_2SO_4(aq) at

open circuit (in-situ). (c) Same as (b) but at an applied potential of -0.300 V vs. SCE (operando). (d) Co standard. (e) CoO standard.

The *ex-situ* spectrum also exhibited a white line feature at 7727 eV similar to that observed for the CoO standard material, indicating the presence of oxidized Co in the as-prepared material that was not present in the active electrocatalyst. After operation and upon exposure to air, the spectrum of the catalyst changed dramatically and was nearly identical to that of aqueous Co^{2+}, indicating the formation of an oxidized hydrate (Figure 5.4). The CoP is therefore stable only under *in-situ* conditions.

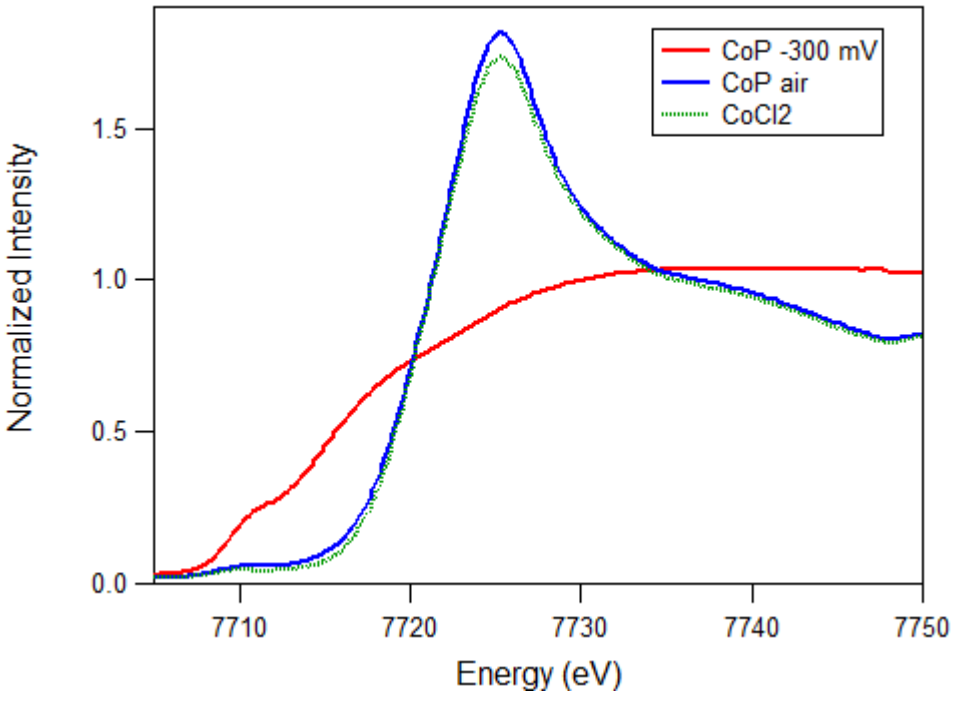

Figure 5.4: Co K-edge XAS of CoP films under the following conditions: (a) spectrum of a CoP film in 0.500 M H_2SO_4(aq) at an applied potential of -0.300 V vs. SCE (*operando*).

(b) spectrum of a CoP film exposed to air after *operando* conditions. (c) Reference spectrum of aqueous $CoCl_2$.

Fourier-transformed Co K-edge EXAFS, presented in Figure 5.5 showed a first-shell distance of ~2.30 Å for the *in-situ* and *operando* catalyst, consistent with reported Co-P distances for amorphous Co-P alloys[11] and crystalline Co_2P.[12] These are longer than the typical Co-O distance of ~2.15 Å (as shown in the CoO standard), implying direct Co-P interactions in the first shell. There was little indication of long range order, consistent with an amorphous catalyst structure as observed by Raman spectroscopy and previously reported results for electrodeposited CoP. The *ex-situ* catalyst displayed a slightly different EXAFS pattern, consistent with a CoP structure mixed with some metallic and oxidized Co as seen by comparison to Co foil and Co oxide standards. After operation and exposure to air, first shell distances were ~0.29 Å shorter, showing a closer match to the CoO standard and consistent with oxidation of Co to form a hydrate.

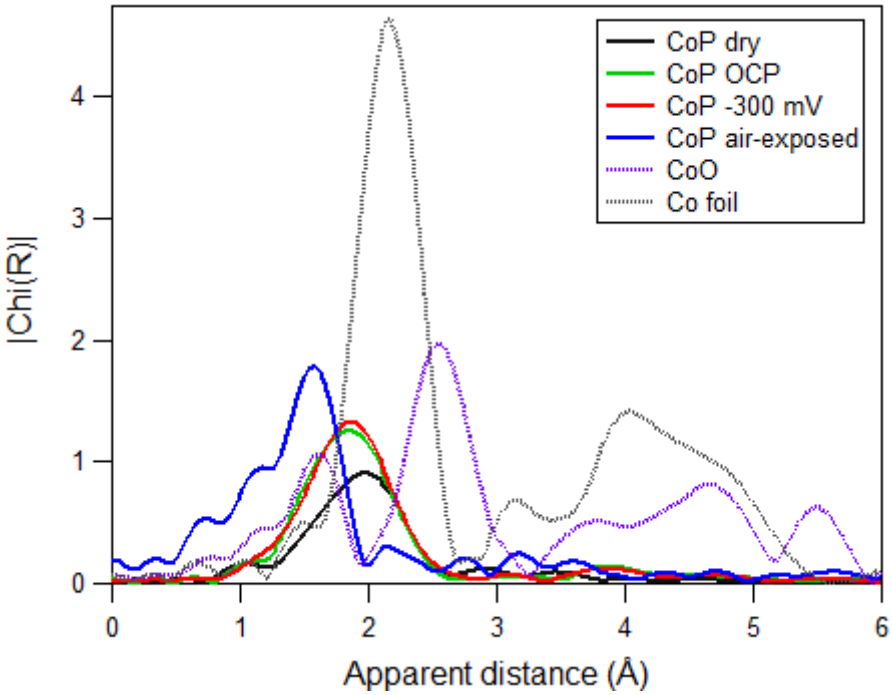

Figure 5.5: Fourier-transformed Co K-edge EXAFS of CoP films under the indicated conditions compared to CoO and Co foil standards, plotted as apparent distance (typically ~0.5 Å shorter than the real distance). (a) Ex-situ spectrum of a CoP film prior to contact with H_2SO_4 electrolyte (air ambient, ex-situ). (b) CoP film in 0.500 M H_2SO_4(aq) at open circuit (in-situ). (c) Same as (b) but at an applied potential of -0.300 V vs. SCE (operando). (d) CoP film after operation and exposure to air. (e) CoO standard. (f) Co foil standard.

Figure 5.6a-c presents P K-edge XAS directly analogous to the Co K-Edge XAS presented in Figure 5.3a-c. P K-edge XAS of K_3PO_4, $NaPO_2H_2$, and GaP standard materials are also shown in Figure 5.6d-f. The *ex-situ* CoP spectrum exhibited three major features which were centered at 2144.9, 2150.2, and 2152.6 eV. The feature at

2144.9 is a close match to that of the GaP standard, and indicates the presence of CoP. The feature at 2152.6 is a close match to the K_3PO_4 standard, and indicates the presence of a phosphate species in the catalyst. The feature at 2150.2 eV should therefore reflect a phosphorous species in oxidation state intermediate between phosphide and phosphate. This feature is close, but not an exact match, to that observed in the $NaPO_2H_2$ standard. Unfortunately, this standard was unstable under the X-ray beam, decomposing into a phosphate species with a characteristic spectral feature near 2152.2 eV, and a phosphide with a characteristic spectral feature near 2144.9 eV (see SI for details). This instability makes it difficult to determine the exact position of the $NaPO_2H_2$ spectral feature, but it appears to be at ~2149.4 eV.

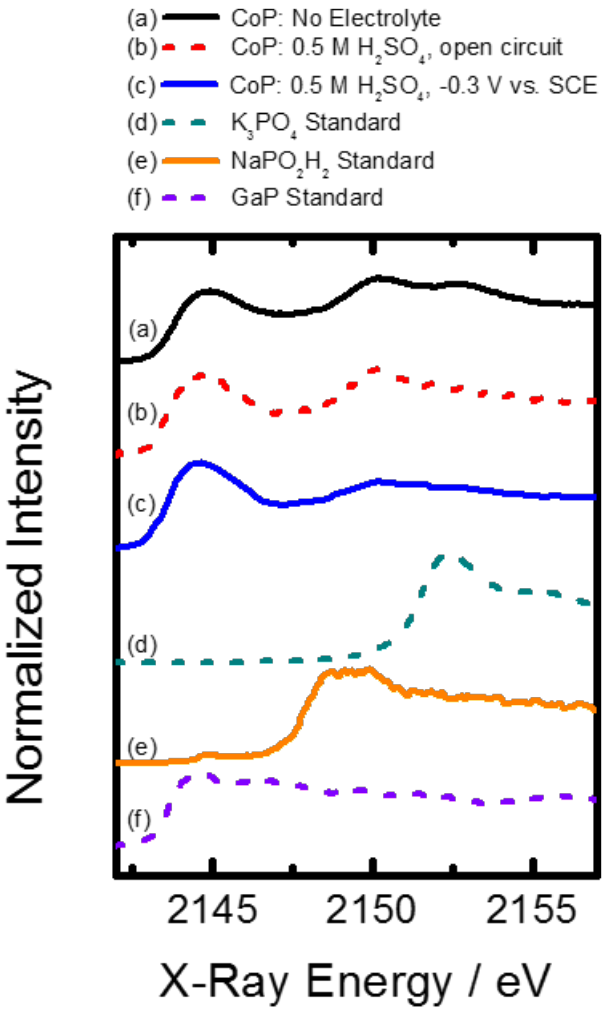

Figure 5.6: P K-edge X-ray absorbance spectra of both CoP films under the indicated conditions and related spectral standards. (a) Ex-situ spectrum of a CoP film prior to contact with H_2SO_4 electrolyte (air ambient, ex-situ). (b) CoP film in 0.500 M H_2SO_4(aq) at open circuit (in-situ). (c) Same as (b) but at an applied potential of -0.300 V vs. SCE (operando). (d) K_3PO_4 standard. (e) $NaPO_2H_2$ standard. (f) GaP standard.

The as-prepared material is therefore composed of P in multiple oxidized and reduced states. Relative to the *ex-situ* spectrum, the spectral features at 2152.6 eV and

2150.2 were attenuated in the *in-situ* and *operando* spectra, but not completely absent, while the feature at 2144.9 (attributed to phosphide) increased in intensity. This behavior is consistent with the Raman analysis, wherein evidence for presence of detectable oxidized P species was only observed in the *ex-situ* examination of the as-prepared material. The cumulative data thus suggest that while *ex-situ* analysis of the electrodeposited film indicates a material composed of multiple phases with Co and P both existing in several oxidation states, the active electrocatalyst is an amorphous material composed of Co in a near-zero valent state and P in a reduced state.

5.3 Conclusion

In summary, CoP films were electrodeposited from an aqueous solution containing $CoCl_2$ and $NaPO_2H_2$. Voltammetric analysis indicated that these films were highly-active catalysts, capable of effecting a -10 mA cm^{-2} current density towards the HER at $-\eta < 100$ mV. *Ex-situ* Raman analysis of as-deposited material indicated the presence of several oxidized Co species, including crystalline Co_3O_4, as well as oxygenated P species but the associated spectroscopic signatures were not observed during *operando* analysis. No phonon scattering was observed during *operando* Raman analysis. Corresponding *ex-situ* Co K-edge and P K-edge XAS also indicated the presence of oxidized Co and P species in addition to a near-zero valent Co species and a reduced P species. The analogous *operando* XAS exhibited disappearance of the absorption edges of oxidized Co and P species. The collective spectroscopic evidence thus indicates that the active electrocatalyst is an amorphous material consisting of Co in a near-zero valent state and P in a reduced state.

5.4 Experimental

Materials and Chemicals All materials and chemicals were used as received from the indicated suppliers without additional purification. H_2O with a resistivity ≥ 18.2 MΩ·cm (Barnstead Nanopure System) was used throughout.

General Electrochemical Details All electrochemistry was performed using a Bio-Logic SP-200 potentiostat and a cell in three-electrode configuration. A saturated calomel electrode (SCE; CH Instruments) was used as the reference electrode. CoP films were electrodeposited on several Cu substrates for the various analytical methods utilized (described below). Films were deposited from an aqueous solution (pH = 5) of 0.20 M $CoCl_2 \cdot 6H_2O$ (99.998%, Alfa Aesar), 0.30 M $NaPO_2H_2 \cdot H_2O$ (97+%, Alfa Aesar), 0.15 M H_3BO_3 (99.99%, Alfa Aesar), and 0.10 M NaCl (99.0+%, Macron Fine Chemicals). Deposition was effected by biasing the Cu electrode potentiostatically at -1.200 V vs. SCE for 0.50 min at room temperature. All analysis was performed in an aqueous solution of 0.500 M H_2SO_4 (A.C.S. Reagent, J. T. Baker). The uncompensated cell resistance (R_u) was determined from a single-point electrochemical impedance measurement obtained by applying a sine-wave modulated potential with an amplitude of 20 mV at a modulation frequency of 100 kHz centered at the open-circuit potential of the cell. Applied potentials during catalyst analysis were dynamically corrected for an uncompensated resistance of 85% of the value of R_u.

Voltammetric Analysis A single compartment cell and a graphite rod counter electrode (99%, Sigma-Aldrich) were utilized for deposition and analysis. Copper disks with a 5 mm diameter and 4 mm thickness (99.999%, Alfa Aesar) were mounted in PTFE

rotating disk electrode tips (Pine Research Instrumentation) and utilized as catalyst substrates for voltammetric experiments. The tips were mounted on a rotator with the tips suspended such that the Cu surface was immersed in deposition solution. After deposition of a CoP film, all electrodes were removed from the cell, and then the electrodes and the cell were rinsed with H_2O. The cell was then refilled with 0.500 M H_2SO_4 electrolyte and the electrodes replaced. Voltammetric data were then obtained by cycling the potential between -0.266 V and -0.406 V vs. SCE at a scan rate of 1 mV s^{-1}.

Raman Spectroscopy Raman spectra were collected with a Renishaw inVia Raman microprobe equipped with a Leica DM 2500 M microscope, a Leica N Plan L 50x objective (numerical aperture = 0.50), a 1800 lines mm^{-1} grating, and a CCD detector configured in a 180° backscatter geometry. A 532 nm diode-pumped solid-state (DPSS) laser (Renishaw RL532C50) was used as the excitation source and a 1.58 mW radiant flux was incident on the surface of the sample. A λ/4 plate was used to circularly polarize the incident excitation. No polarizing collection optics were used. ~ 1 cm square Cu foil (99.9999%, Alfa Aesar) sections were utilized as catalyst substrates for Raman experiments. Single-compartment O-ring compression cells that confined the contact area between the electrolyte and the Cu foil to a circular area of 0.1 cm^2, and graphite rod counter electrodes, were used for deposition and analysis. After deposition of a CoP film, the Cu foil section was removed from the deposition cell, rinsed with H_2O and dried under a stream of N_2(g). *Ex-situ* Raman spectra were then acquired. The CoP-decorated Cu foil was then placed in the analysis cell with 0.500 M H_2SO_4. The O-ring seal was located on the bottom wall of the analysis cell. The cell was equipped with a glass window on the top face that enabled *in-situ* and *operando* collection of Raman signal.

Raman spectra were acquired *in-situ* after solution was added to the cell. The CoP film was then conditioned by cycling the potential 10 times between -0.266 V and -0.406 V vs. SCE at a scan rate of 15 mV s^{-1}. Raman spectra were then obtained under *operando* conditions by acquiring spectra while the electrode was under potential control.

X-ray Absorption Spectroscopy Co K-edge X-ray absorption spectra (XAS) were performed at Beamline 7-3 at the Stanford Synchrotron Radiation Lightsource (SSRL) at SLAC National Accelerator Laboratory. Monochromatic incoming radiation was obtained using a Si(220) double crystal that had been detuned to 50% of the flux maximum at the K-edge, to attenuate higher harmonics. The incident beam intensity was monitored by a N_2-filled ionization chamber that was positioned between the source and the sample. Fluorescence signal was collected at 90 degrees from the source propagation vector using a 30-element Ge detector (Canberra Industries). P K-edge XAS measurements were performed at Beamline 14-3 at the SSRL. Monochromatic X-rays were produced using a Si(111) double crystal. The incident radiation intensity was monitored via a He-filled ionization chamber that was positioned between the source and the sample. Fluorescence signal was collected at 90 degrees from the source propagation vector using a Vortex 4-element silicon drift detector (Hitachi High-Technologies Science).

Ex-situ Co K-Edge XAS of Co and CoO (99.998%, Alfa Aesar) and P K-Edge XAS of $K_3PO_4 \cdot 7H_2O$ (98%, VWR), $NaPO_2H_2 \cdot H_2O$ (99%, Sigma Aldrich) and GaP were acquired as standards. Powder standards (all except for Co and GaP) were diluted with BN to minimize overabsorption effects. P K-edge XAS were acquired under a He ambient to prevent atmospheric X-ray attenuation.

3 mm square, 0.5 μm thick Si_3N_4 membranes, enclosed by a 10 mm square Si frame, were utilized as X-ray transparent substrates. Electron-beam evaporation was used to deposit a 2 nm thick Ti adhesion layer and a 100 nm Cu film on one side of the framed Si_3N_4 membranes. A deposition rate of 2 Å s^{-1}, with the base pressure 5 x 10^{-6} Torr and a substrate temperature of 100 °C were utilized. A two compartment H-cell was utilized for deposition and analysis, as described elsewhere.[13, 14] Briefly, a porous glass frit was used to divide the two compartments. An Ir foil (99.7%, Goodfellow) counter electrode was utilized and isolated in one of the two compartments. The reference electrode was placed in the other compartment. The compartment that housed the reference electrode had a square opening. The framed, Cu-coated Si_3N_4 membranes were affixed to the cell in this location by use of epoxy, with the Cu-coated portion of the electrode facing into the cell (Loctite Instant Mix). After deposition of a CoP film, the counter and reference electrodes were removed from the cell, and then the electrodes and the cell were rinsed with H_2O. *Ex-situ* XAS of the CoP films were then acquired. During XAS acquisition, the excitation X-rays were directed at 45 degrees to the exposed Si_3N_4 face. For the P K-edge XAS experiments, the entire cell was enclosed in a He-filled bag to prevent atmospheric X-ray attenuation. After collection of the *ex-situ* spectra, the cell was refilled with 0.500 M H_2SO_4(aq) and the electrodes were replaced. The CoP film was then conditioned by cycling the potential 10 times between -0.266 V and -0.406 V vs. SCE at a scan rate of 15 mV s^{-1}. XAS were then obtained under *operando* conditions while the electrode was under potentiostatic control.

Spectra were subjected to baseline correction and intensity normalization using the Athena software package based on IFEFFIT.[15, 16] For the CO K-edge EXAFS, the

background was fit using a five-domain cubic spline and removed, and the resulting oscillations were plotted in k-space and then Fourier-transformed into real space for analysis.

5.5 References

1. F. H. Saadi, A. I. Carim, E. Verlage, J. C. Hemminger, N. S. Lewis and M. P. Soriaga, *J. Phys. Chem. C*, 2014, **118**, 29294-29300.

2. J. Tyczkowski, R. Kapica and J. Łojewska, *Thin Solid Films*, 2007, **515**, 6590-6595.

3. V. G. Hadjiev, M. N. Iliev and I. V. Vergilov, *J. Phys. C Solid State Phys.*, 1988, **21**, L199-L201.

4. R. L. Frost, Spectrochim. Acta Mol. Biomol. Spectrosc., 2004, **60**, 1439-1445.

5. P. C. H. Mitchell, S. F. Parker, K. Simkiss, J. Simmons and M. G. Taylor, *J. Inorg. Biochem.*, 1996, **62**, 183-197.

6. R. M. Bell and M. A. Jeppesen, *J. Chem. Phys.*, 1935, **3**, 245.

7. R. A. Cox, Ü. L. Haldna, K. L. Idler and K. Yates, *Can. J. Chem.*, 1981, **59**, 2591-2598.

8. M. Pourbaix, Atlas of Electrochemical Equilibria In Aqueous Solutions, Permagon Press, Oxford, 1966.

9. K. K. Bando, T. Wada, T. Miyamoto, K. Miyazaki, S. Takakusagi, Y. Koike, Y. Inada, M. Nomura, A. Yamaguchi, T. Gott, S. Ted Oyama and K. Asakura, *Journal of Catalysis*, 2012, **286**, 165-171.

10. T. Kawai, S. Sato, W. Chun, K. Asakura, K. Bando, T. Matsui, Y. Yoshimura, T. Kubota, Y. Okamoto and Y. Lee, *Physica Scripta*, 2005, **2005**, 822.

11. G. CARGILL III and R. Cochrane, *Le Journal de Physique Colloques*, 1974, **35**, C4-269-C264-278.

12. S. Rundqvist, *Acta Chem. Scan*, 1960, **14**, 1961-1979.

13. Y. Gorlin, B. Lassalle-Kaiser, J. D. Benck, S. Gul, S. M. Webb, V. K. Yachandra, J. Yano and T. F. Jaramillo, *J. Am. Chem. Soc.*, 2013, **135**, 8525-8534.

14. S. Gul, J. W. Ng, R. Alonso-Mori, J. Kern, D. Sokaras, E. Anzenberg, B. Lassalle-Kaiser, Y. Gorlin, T. C. Weng, P. H. Zwart, J. Z. Zhang, U. Bergmann, V. K. Yachandra, T. F. Jaramillo and J. Yano, *Phys. Chem. Chem. Phys.*, 2015, **17**, 8901-8912.

15. B. Ravel and M. Newville, *Journal of synchrotron radiation*, 2005, **12**, 537-541.

16. M. Newville, *Journal of synchrotron radiation*, 2001, **8**, 322-324.